Multiband Band and Dual Diversity Eight-Element MIMO Microstrip Antenna for Wireless Applications

Ater David Utahile [a], Udofia Kufre Michael [a*] and Obot Akaninyene Bernard [a]

[a] *Department of Electrical and Electronics Engineering, University of Uyo, Uyo, Nigeria.*

Authors' contributions

This work was carried out in collaboration among all authors. All authors read and approved the final manuscript.

Original Research Article

ABSTRACT

This paper presents the design and performance analysis of multiband dual diversity 8-element multiple-input multiple-output (MIMO) antenna at 2.45/3.5/5.2/6 GHz. The proposed antenna was designed on a Flame Resistant (FR-4) substrate having a dielectric constant of 4.4 ($\varepsilon_r = 4.4$), dimensions of $200 \times 200 \times 1.6\ mm$. The antenna was simulated and analyzed using Computer Simulation Studio (CST Studio). Results obtained from simulation showed that the 8-element MIMO antenna achieved a combined bandwidth of 908.68 MHz representing 34.51% of the fractional bandwidth. Broadside radiation pattern was observed across the three frequency bands in both E- and H-plane with average main lobe magnitude of 7.8 dBi. Furthermore, proposed antenna achieved consistent Envelop Correlation Coefficient (ECC) and Diversity Gain (DG) values of 0.0008 and 9.999 as well as Port-to-port isolation of 27 dB across all frequencies considered. Also, an antenna gain of 8.58 dB was achieved at a frequency of 6 GHz. The gain, isolation, DG and ECC between adjacent ports as well as the loss in capacity were within the standard margins, making the antenna structure suitable for MIMO applications.

_____

Corresponding author: Email: kufremudofia@uniuyo.edu.ng;

1. INTRODUCTION

Since the addition of Multiple Input Multiple Output (MIMO) technology by the Third Generation Partnership Progress (3GPP) in the year 2008 to their Release 8 that also saw the introduction of Long-Term Evolution (LTE) Standard, substantial progress was not made in the practical deployment of the technology until recently [1]. MIMO technology, according to Cheng et al. [2], is defined as is a wireless technology that increases the data capacity of a Radio Frequency (RF) channel by using multiple transmitting and receiving antennas. Two broad categories of MIMO technology generally known are Single User MIMO (SU-MIMO) and Multi-User MIMO (MU-MIMO) [3]. The former refers to the adoption of multiple transmitting antennas and a receiver for communication while the latter is the adoption of multiple antennas at either end of the communication link. The adoption of MIMO technique in wireless communication was borne out of the desire to overcome the difficulties associated with single antenna transmission system at the inception of the LTE communication standard in order to take advantage of beamforming gain, spatial/ polarization diversity and spatial multiplexing [4]. Chattha in his submission in [5], stated that MIMO technology uses multipath to achieve higher data rates This improved data rates simultaneously increased reliability and range without using extra bandwidth thereby improving spectral efficiency to cope with the need for high data rates for different services. Ref [5] added that antenna diversity is one of the prominent techniques used in cubbing multipath fading in no clear Line-of-Sight (LoS) radio channel in that it implements either spatial, pattern or polarization diversity or a combination of these. By interpretation, Jamshed et al. [6] highlighted that to fully explore diversity gain for 5G communication, more than one diversity scheme implementation was recommended and this was only achievable with a multi-element antenna configuration.

Microstrip antenna has been explored by several authors as a viable option in the deployment of MIMO technology. Shoaib et al. [7] presented the design of MIMO antennas for mobile handsets covering GSM 1800/1900 band, Wireless Local Area Network (WLAN) and some LTE bands. Nithya et al. [8] proposed an eight element MIMO antenna for 5G smartphones which resonated at 3.8, 4.5 and 5.8 GHz. Closely mounted mobile handset MIMO antenna for LTE 13 band application was presented by Lee et al [9]. Though these publications met their different outlined objectives, they however did not optimize for the frequency range considered in this study.

In this paper, an 8-element MIMO antenna is presented for multifrequency application including C-band 5G deployment frequency for the Nigerian market as well as frequencies for Wireless Fidelity (WiFi) and WiFi 6 standards as put forward by the Institute of Electrical Electronics Engineering (IEEE). Four single band microstrip antennas resonating at 2.45, 3.5, 5.2, and 6 GHz were designed with readily available transmission line equations. The patches were arranged in pairs at right angles on each side of a flame Resistant (FR-4 Epoxy) substrate.

2. METHODOLOGY

The design of four single band antennas at 2.45, 3.5, 5.2 and 6 GHz center frequencies is preceded by that of the MIMO antenna consisting of two elements of the single band antenna for each frequency band considered.

2.1 Antenna Design

The design of the constituent single band microstrip antennas follows the transmission line equations for designing rectangular antennas from [10]. The basic parameters of the microstrip such as the width, length and the dimensions of the microstrip line are determined as follows:

The width of the patch W_p is determine from Equation 1:

$$W_p = \frac{c}{2f_r} \sqrt{\frac{2}{\varepsilon_r + 1}} \qquad (1)$$

Where c, f_r and ε_r are the speed of light, design frequency and relative permittivity.

The patch length was calculated using Equation 4, however, the length's extension, ΔL and the effective permittivity, ε_{reff} are first calculated from Equations 2 and 3 before determining the length of the microstrip patch. The substrate thickness, h of 1.6 mm was maintained all through the

design. The effective dielectric constant and length extension are calculated thus:

$$\varepsilon_{reff} = \frac{\varepsilon_r+1}{2} + \frac{\varepsilon_r-1}{2}\left[1+12\frac{h}{W_p}\right]^{-\frac{1}{2}} \qquad (2)$$

$$\Delta L = 0.412h \frac{(\varepsilon_{reff}+0.3)\left[\frac{W_p}{h}+0.264\right]}{(\varepsilon_{reff}-0.258)\left[\frac{W_p}{h}+0.8\right]} \qquad (3)$$

The patch length was calculated from Equation 4 thus:

$$L = \frac{c}{2f_r\sqrt{\varepsilon_{reff}}} - 2\Delta L \qquad (4)$$

As earlier stated, inset feeding technique was used in order to offset the feeding location to the point where impedance match between the patch and feedline can be achieved. The inset feed parameters were determined using Equations 5 to 7.

To calculate the notch width, g, equation for the notch width from [11] was employed as given in Equation 5.

$$g = \frac{c\, f_r \times 10^{-9} \times 4.65 \times 10^{-9}}{\sqrt{2\varepsilon_{reff}}} \qquad (5)$$

The resonant input resistance R_{in} was calculated from Equation 6:

$$R_{in}(y=y_o) = \frac{1}{2(G_1+G_{12})}\cos^2\left(\frac{\pi y_o}{L_p}\right) \qquad (6)$$

The equation for the characteristic impedance Z_o is given in Equation 7;

$$Z_0 \begin{cases} \frac{60}{\sqrt{\varepsilon_{reff}}}\ln\left[\frac{8h}{W_f}+\frac{W_f}{4h}\right] & \frac{W_f}{h}\leq 1 \\ \frac{120\pi}{\sqrt{\varepsilon_{reff}}}\left[\frac{W_f}{h}+1.393+0.667\ln\left(\frac{W_f}{h}+1.444\right)\right] \end{cases} \qquad (7)$$

In this design, the ratio, $\frac{W_f}{h} = \frac{2.98}{1.6} = 1.863 > 1$, so the second expression in Equation 7 applies.

Edge impedance, $R_{in(edge)}$ is computed from Equation 8.

$$R_{in(edge)} = \frac{1}{2(G_1 \mp G_{12})} \qquad (8)$$

As reported by Balanis [10], the plus (+) sign is used for modes with odd (antisymmetric) resonance voltage distribution beneath the patch and between the slots while minus (-) sign is used for modes with even symmetric resonant voltage distribution. In order to evaluate the input resistance, other parameters such as wave number k, input current I_1, input conductance G_1 and mutual conductance G_{12} have to be known first. The equations for computing the various parameters highlighted are given in Equations 9 to 13.

$$k = \frac{2\pi}{\lambda_{air}} \qquad (9)$$

$$I_1 = -2 + \cos(X) + XS_i(X) + \frac{\sin(X)}{X} \qquad (10)$$

$$X = kW_p \qquad (11)$$

$$G_1 = \frac{I_1}{120\pi^2} \qquad (12)$$

$$G_{12} = \frac{1}{120\pi^2}\int_0^\pi \left[\frac{\sin\left(\frac{kW_p}{2}\cos\theta\right)}{\cos\theta}\right]^2 J_o(kL_p\sin\theta)\sin^3\theta d\theta \qquad (13)$$

Where J_o is the Bessel function of the first kind of order zero. G_{12} was resolved using MATLAB-based program developed for the calculation of rectangular microstrip antenna parameters [12].

Inset feed technique is used with a chosen characteristic impedance of 50 Ω.

To calculate the inset feed recessed distance, y_o and the width of the transmission line, W_f Equations 15 and 16 are used.

$$Z_o = R_{in(edge)}\cos^2\left(\frac{\pi}{L_p}y_0\right) \qquad (14)$$

$$y_0 = \frac{L_p}{\pi}\cos^{-1}\left[\sqrt{\frac{Z_0}{R_{in(edge)}}}\right] \qquad (15)$$

According to Pozar [11], the width of the transmission line is calculated thus; For $\frac{W_f}{h} > 2$;

$$W_f = \left(\frac{2h}{\pi}\right) \times \left[\frac{60\pi^2}{Z_o\sqrt{\varepsilon_r}}-1-\ln\left[2\times\left[\frac{60\pi^2}{Z_o\sqrt{\varepsilon_r}}\right]-1\right]+\left(\frac{\varepsilon_r-1}{2\varepsilon_r}\right)\times\left(\ln\left[\left[\frac{60\pi^2}{Z_o\sqrt{\varepsilon_r}}\right]-1\right]+0.39-\frac{0.61}{\varepsilon_r}\right)\right] \qquad (16)$$

Ideally, an infinite ground plane is desired for patch antennas but for want of space and reduced device size, the minimum ground plane dimensions for optimal performance was calculated using Equations 17 and 18 thus:

The length of the ground plane (L_g) is:

$$L_g = 6h + L_p \qquad (17)$$

The width of the ground plane is:

$$W_g = 6h + W_p \qquad (18)$$

Dielectric constant (ε_r) = 4.4, Substrate height (h) = 1.6 mm, Patch thickness (t) = 0.035 mm, Characteristic impedance of the feed line (Z_0) = 50 Ω.

The computed values are presented in Table 1 while the geometry of the designed single band RMSAs is depicted in the schematic diagram is presented in Fig. 1.

In combining multiple elements on a single substrate, the challenge of mutual coupling of antenna elements arises due to the simultaneous reflections at similar frequencies [13]. However, as stated by Garg et al. [14], to lower the risk of mutual coupling, maintain single mode propagation among radiating elements, and to have in-phase element characteristics as well as radiation in normal direction, the distance between elements is approximated to be about half wavelength $\left(\frac{\lambda_{air}}{2}\right)$; thus,

$$\text{Patch spacing, (d)} = \frac{\lambda_{air}}{2} = \frac{85.71}{2} = 42.90 \; mm.$$

Another notable reason why a good separation distance, d, is necessary is that it enhances the ability to introduce space diversity within the antenna integrated device. Saurabh et al. [15] proposed the orthogonal placement of antenna elements with a view to achieving high isolation especially with interconnected ground plane, this idea was adopted for the placement of antenna elements during the design of the proposed MIMO antenna. Hence, for the proposed design, pair of each adjourning single band antenna element will be placed orthogonally (at right angle) to the next with the opposite elements positioned in a reversed order (at an angle of 180^0). With this approach, polarization diversity (linear and circular polarization) is easily achieved as depicted in Fig. 3. The substrate dimensions are $120 \times 120 \times 1.6 \; mm$ for the 4-element MIMO antenna and $200 \times 200 \times 1.6 \; mm$ for the 8-element MIMO antenna.
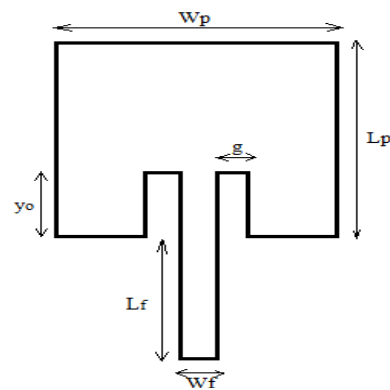
Fig. 1. Geometry of the designed antenna

Four rectangular single band antennas designed at 2.45 GHz, 3.5 GHz, 5.2 GHz and 6 GHz in CST Microwave Studio are presented in Fig. 2. Each antenna is fed with a 50Ω feedline emanating from a wave port at the edge of the substrate. Also, 4-element multi-frequency antenna and 8-element multiband MIMO antenna incorporating the single band antennas designed at the various frequencies of interest are presented in Fig. 3 and Fig. 4.

Table 1. Design dimensions of single band inset-fed RMSAs

| Design parameter	2.45 GHz	3.5 GHz	5.2 GHz	6 GHz
Patch dimensions				
Length (L_p)	28.83 mm	20.22 mm	13.20 mm	11.33 mm
Width (W_p)	37.26 mm	26.08 mm	17.56 mm	15.21 mm
Ground plane dimensions				
Length of ground plane (L_g)	38.43 mm	29.82 mm	22.80 mm	20.93 mm
Width of ground plane (W_g)	46.86 mm	35.68 mm	27.16 mm	24.81 mm
Feed line dimensions				
Width of inset feed (W_f)	3.10 mm	3.10 mm	3.02 mm	3.02 mm
Inset distance (y_0)	10.69 mm	7.41 mm	4.89 mm	3.76 mm
Inset gap (g)	1.20 mm	1.73 mm	1.53 mm	1.56 mm
Length of 50 Ω transmission line (L_f)	4.80 mm	4.80 mm	4.80 mm	4.80 mm
Input edge impedance of the patch (R_{in})	320.11 Ω	319.21 Ω	317.60 Ω	316.33 Ω
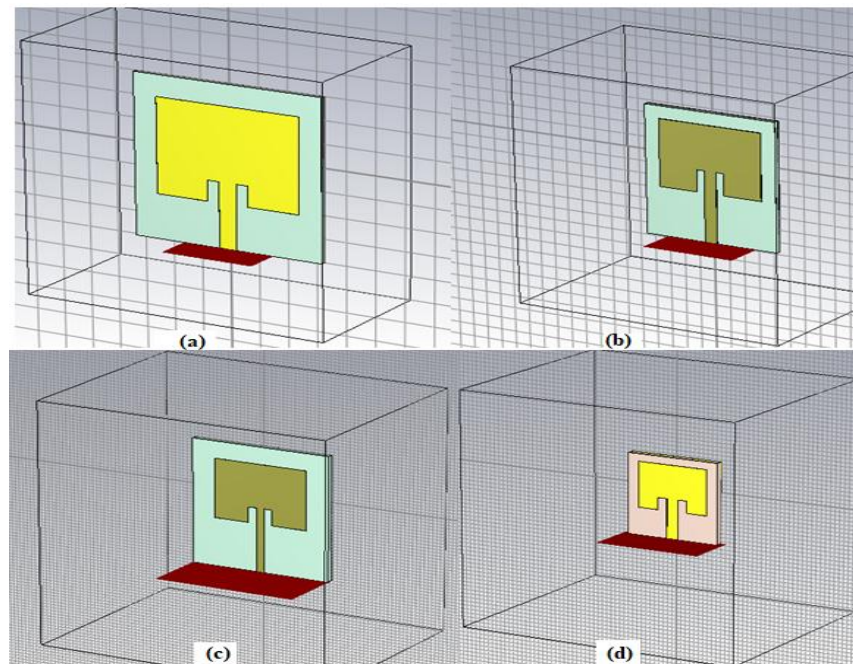
Fig. 2. Designed single band antenna (a) at 2.45 GHz (b) at 3.5 GHz (c) at 5.2 GHz (d) at 6 GHz
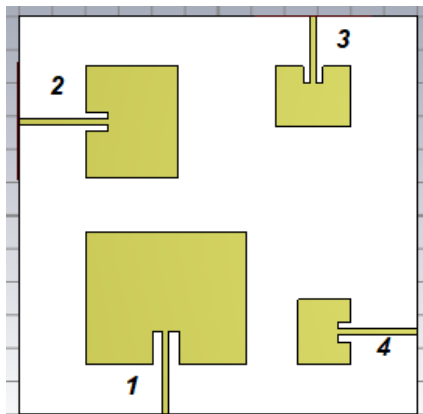

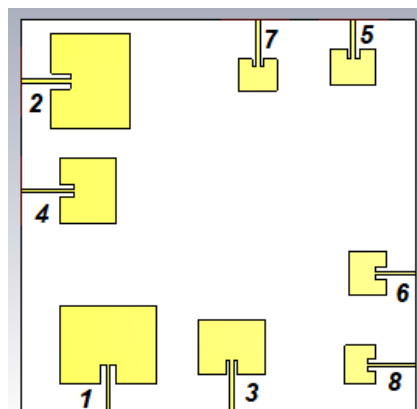**Fig. 3. Multi-frequency 4-element antenna**

**Fig. 4. Dual diversity 8-element multi-frequency MIMO antenna**

3. RESULTS AND DISCUSSION

Antenna parameters generally used for antenna analysis like s-parameters, impedance bandwidth, VSWR, gain, directivity and current distribution of all antennas designed in the previous section are presented in this section. The S-parameter achieved by the 8-element antenna at 2.45 GHz (S_{11} and S_{22}), 3.5 GHz (S_{33} and S_{44}), 5.2 GHz (S_{55} and S_{66}) and 6 GHz (S_{77} and S_{88}) are presented in Fig. 5 to Fig. 8. The depicted S-parameters (S_{mn}) designations correspond to typical S_{11} parameter of single element antenna. Fig. 9 gives the combined return loss plot consisting of all antenna elements. Worthy of note however, is that on all the S-parameter plots presented, minimum return loss of -36.46 was obtained at resonance frequency of 5.2 GHz.

Another notable feature observed from the return loss property illustrated in Fig. 9 is the somewhat consistency of narrow bandwidth recorded at all frequencies of interest which affirms the lack of relationship between increased microstrip antenna element and bandwidth improvement.

The radiation pattern in E- and H-plane of the 8-element MIMO antenna at 2.45/3.5/5.2/6 GHz are presented in Fig. 10 to Fig. 13. The H-plane radiation properties are illustrated in Fig. 10 and Fig. 11 from which a nearly omnidirectional pattern was observed at 5.2 GHz. Similarly, the
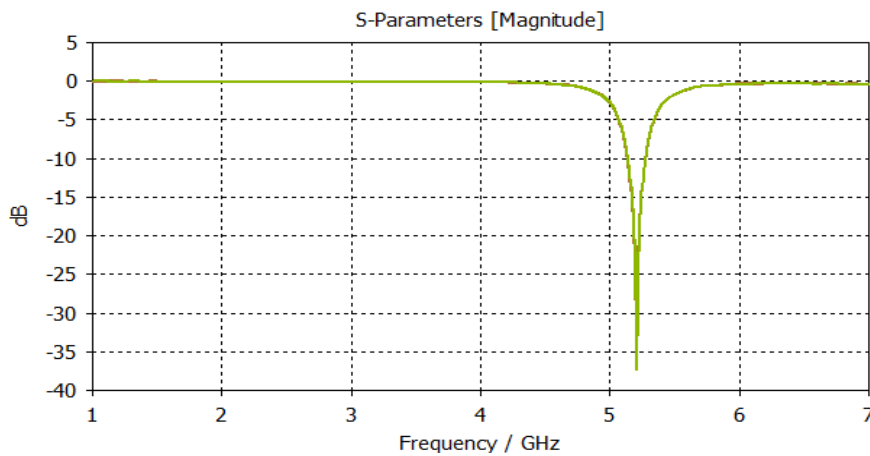
E-plane pattern are presented in Fig. 12 and Fig. 13. Notable characteristic of all the radiation pattern shown is the consistent broadside radiation pattern across the designed frequencies with average main lobe magnitude of 7.8 dBi.
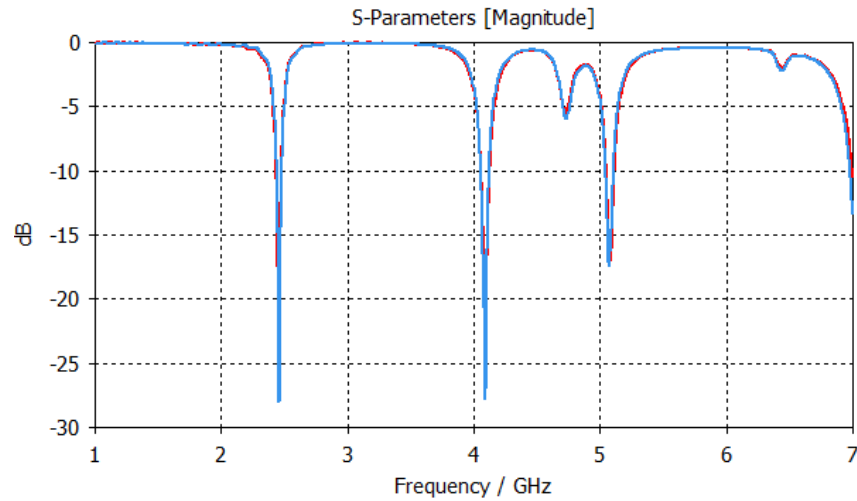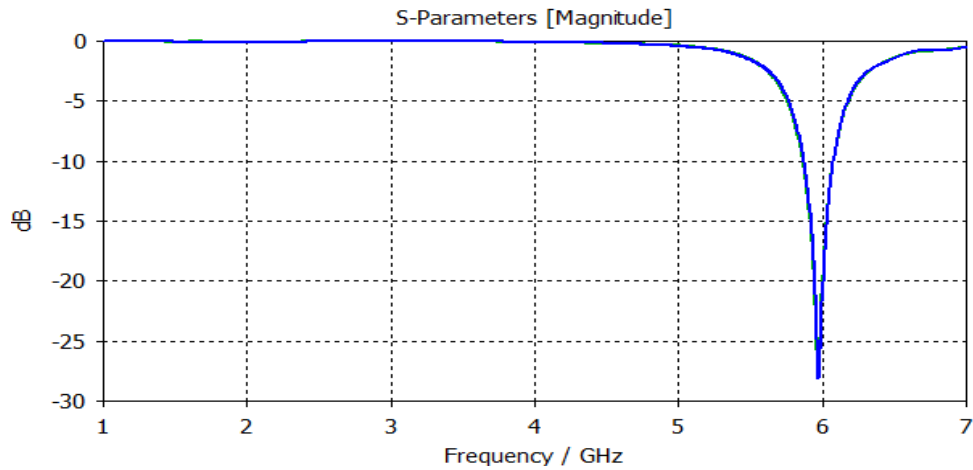

Fig. 5. S-parameter of proposed antenna at 2.45 GHz (S_{11} and S_{22})
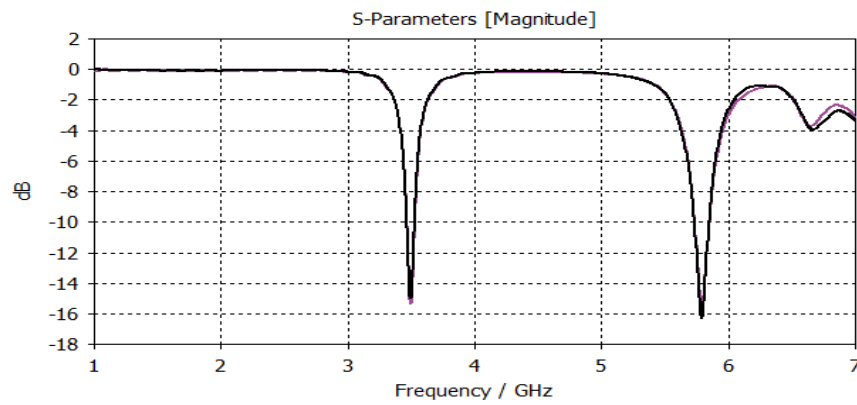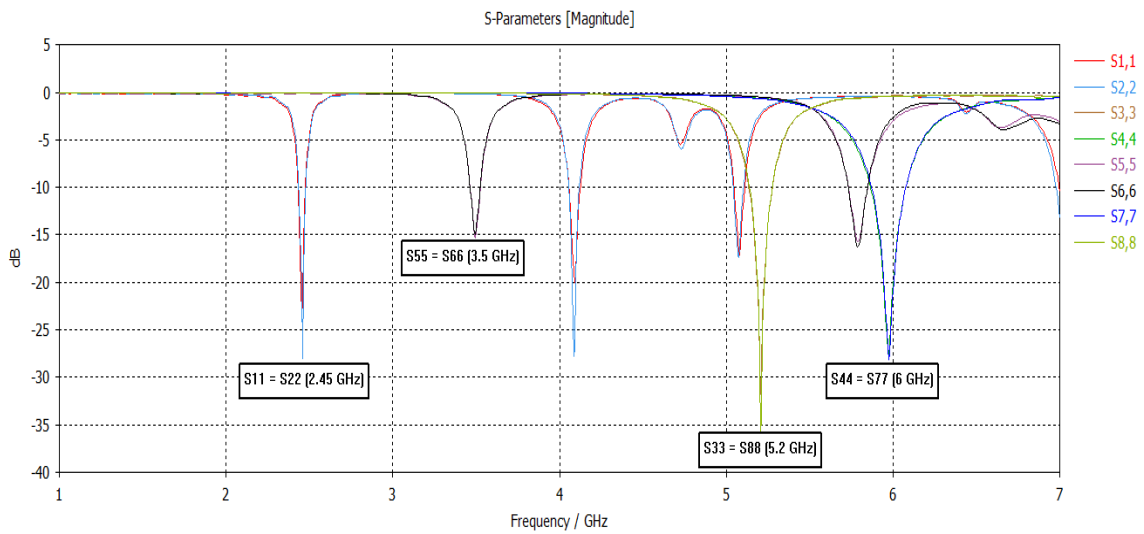

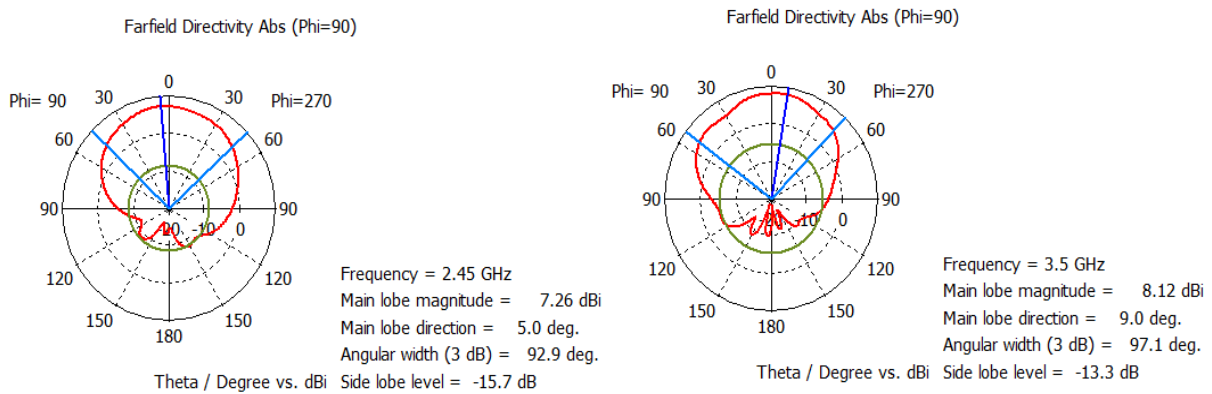**Fig. 6. S-parameter of proposed antenna at 3.5 GHz (S_{33} and S_{44})**

Fig. 7. S-parameter of proposed antenna at 5.2 GHz (S_{55} and S_{66})

Fig. 8. S-parameter of proposed antenna at 6 GHz (S_{77} and S_{88})

Fig. 9. S-parameter of proposed antenna showing all designed frequencies

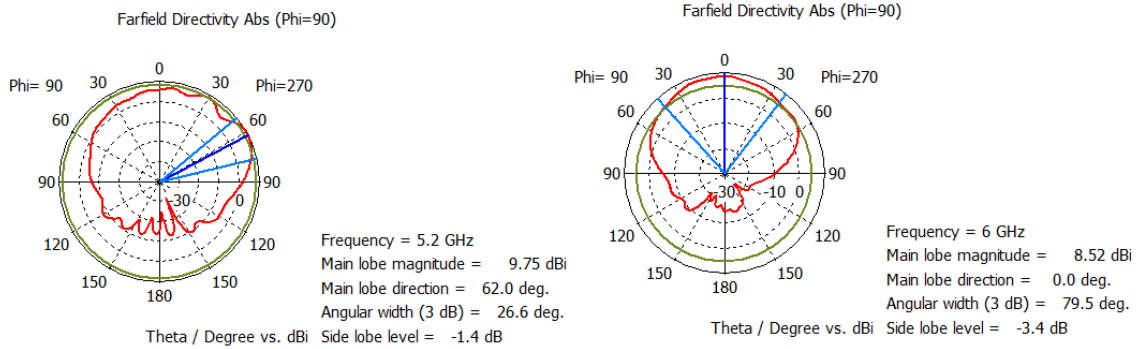**Fig. 10. E-plane of proposed antenna at 2.45 and 3.5 GHz**

Farfield Directivity Abs (Phi=90)

Phi= 90   Phi=270

Frequency = 5.2 GHz
Main lobe magnitude =   9.75 dBi
Main lobe direction =   62.0 deg.
Angular width (3 dB) =   26.6 deg.
Theta / Degree vs. dBi   Side lobe level =   -1.4 dB

Farfield Directivity Abs (Phi=90)

Phi= 90   Phi=270

Frequency = 6 GHz
Main lobe magnitude =   8.52 dBi
Main lobe direction =   0.0 deg.
Angular width (3 dB) =   79.5 deg.
Theta / Degree vs. dBi   Side lobe level =   -3.4 dB

Fig. 11. E-plane of proposed antenna at 5 and 6 GHz

Farfield Directivity Abs (Phi=0)

Phi= 0   Phi=180

Frequency = 2.45 GHz
Main lobe magnitude =   7.23 dBi
Main lobe direction =   5.0 deg.
Angular width (3 dB) =   82.7 deg.
Theta / Degree vs. dBi   Side lobe level =   -14.7 dB

Farfield Directivity Abs (Phi=0)

Phi= 0   Phi=180

Frequency = 3.5 GHz
Main lobe magnitude =   8.22 dBi
Main lobe direction =   8.0 deg.
Angular width (3 dB) =   74.4 deg.
Theta / Degree vs. dBi   Side lobe level =   -19.3 dB

Fig. 12. H-plane of proposed antenna at 2.45 and 3.5 GHz

Farfield Directivity Abs (Phi=0)

Phi= 0   Phi=180

Frequency = 5.2 GHz
Main lobe magnitude =   8.31 dBi
Main lobe direction =   35.0 deg.
Angular width (3 dB) =   32.1 deg.
Theta / Degree vs. dBi   Side lobe level =   -0.7 dB

Farfield Directivity Abs (Phi=0)

Phi= 0   Phi=180

Frequency = 6 GHz
Main lobe magnitude =   8.85 dBi
Main lobe direction =   59.0 deg.
Angular width (3 dB) =   35.1 deg.
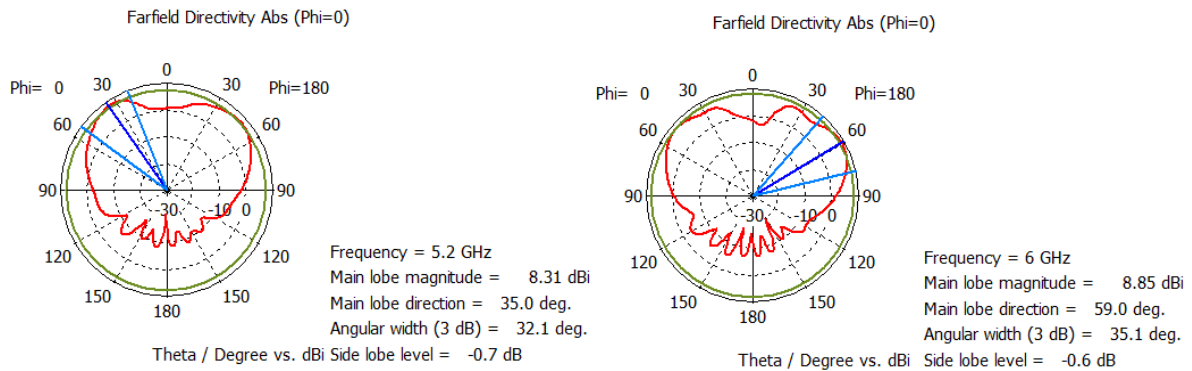Theta / Degree vs. dBi   Side lobe level =   -0.6 dB

Fig. 13. H-plane of proposed antenna at 5 and 6 GHz

The Envelope Correlation Coefficients (ECC) and Diversity Gain (DG) of the 8-element multi-frequency MIMO antenna are presented in Fig. 14 and Fig. 15. At every frequency considered, the proposed antenna averaged ECC and DG values of 8.22×10^{-4} and 9.9999.

A brief comparison of ECC and port isolation of the proposed antenna and some selected literatures is presented in Table 2. The antennas presented in this study is observed to offer better ECC and port isolation especially at 6 GHz.

Table 2. Antenna gain of proposed antennas

Antenna	ECC	Port Isolation
[5]	0.009	13
[6]	0.005	15
[15]	0.014	21
4-element MIMO	0.0008	33
8-element MIMO	0.000081	27

Also, the antenna gains achieved by the studied antennas were compared with other published works as presented in Table 3. In comparing the

proposed antenna with that presented by Saurabh et al. [15], it is observed that the antennas proposed achieved comparable antenna gain at higher frequencies of 5.2 and 6 GHz in both the 4-element and 8-element antenna. Also, in terms of size the antennas proposed by Hua et al. [16] especially the variant with reflector occupies a larger footprint ($220 \times 220 \times 100\ mm$) when compared to the 8-element MIMO antenna ($200 \times 200 \times 1.6\ mm$) proposed in this study. Comparison of proposed MIMO antennas with reviewed works in terms of ECC and port isolation is summarized in Table 3.
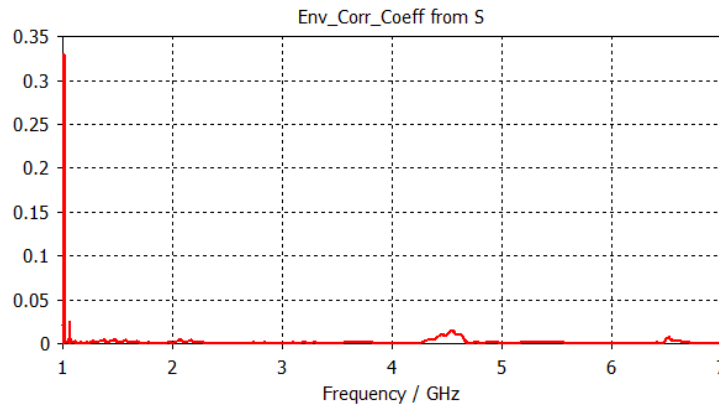

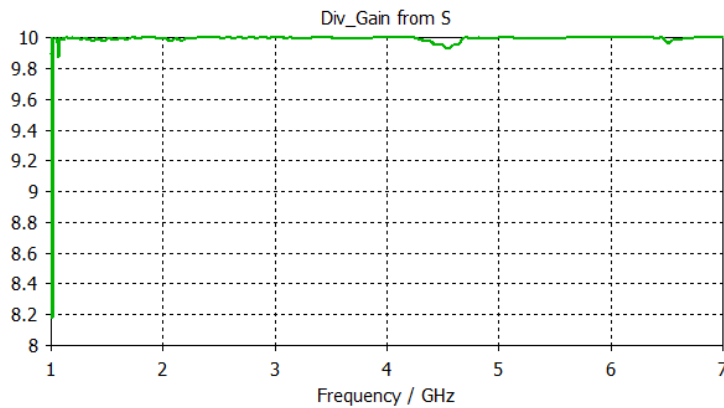**Fig. 14. ECC of proposed 8-element MIMO antenna**

Fig. 15. DG of proposed 8-element MIMO antenna

Table 3. Antenna gain of proposed antennas

Antenna	Frequency (GHz)	Gain (dB)
[16]	3.3 – 3.8	8.5
[17]	3.4 - 3.65	4.8
[18]	3.4 – 3.65	2.87
[19]	3.25 – 3.65	3.90
[20]	3.4 – 3.6	2.5
4-element MIMO	2.45	6.92
	3.50	6.67
	5.20	7.78
	6.00	7.97
8-element MIMO	2.45	7.26
	3.50	7.43
	5.20	8.23
	6.00	8.58

4. CONCLUSION

In this study, six antennas - four single band RMSAs (2.45 GHz, 3.5 GHz 5.2 GHz and 6 GHz), 4-element multiband antenna and 8-element multiband dual diversity MIMO antenna – have been designed, simulated and analyzed, clarifications have been made on several parameters such as return loss, gain, directivity and radiation pattern as well as ECC and DG for MIMO antenna. From simulation results, a combined bandwidth of 908.68 MHz, average antenna gain of 6.2 dB and DG of 9.9995 were achieved at all design frequencies considered for the 8-element MIMO antenna. The number of frequency bands covered by the MIMO antenna presented in this study qualifies it for multiple wireless applications.

COMPETING INTERESTS

Authors have declared that no competing interests exist.

REFERENCES

1. Aldmour I. LTE and WiMAX: Comparison and future perspective. Commun. Netw. 2013;5(4):360–368.
2. Cheng Y, Lu J, Sheng B. MIMO handset antenna for 5G/WLAN applications. Frontiers of Information Technology and Electronic Engineering. 2020;21(1)182–187.
3. Schwarz S, Heath RW, Rupp M. Single-user MIMO versus multi-user MIMO in distributed antenna systems with limited feedback. EURASIP J. Adv. Signal Process. 2013;(1), 54.
4. Dahlman E, Stefan P, Skold J. 4G, LTE-Advanced Pro and The Road to 5G, Third. London, UK: Academic Press; 2016.
5. Chattha HT. 4-Port 2-Element MIMO antenna for 5G portable applications. IEEE Access. 2019;7(4):96516–96520.
6. Jamshed MA, Ur-Rehman M, Frnda J, Althuwayb AA, Nauman A, Cengiz K. Dual band and dual diversity four-element MIMO dipole for 5G handsets. Sensors. 2021:1–13.
7. Shoaib S, Shoaib I, Shoaib N, Chen X, Parini CG. MIMO antennas for mobile handsets. IEEE Antennas Wirel. Propag. Lett. 2015;X(c):1–4.
8. Nithya S, Sandhiya M, Kumar RS, Vaishnavi S, Prasad SRV. Design and fabrication of microstrip MIMO antenna for 5G smart phones. J. Phys. Conf. Ser. 2021;1916(1):1-5.
9. Lee B, Harackiewicz FJ, Wi H. Closely mounted mobile handset MIMO antenna for LTE 13 band application. IEEE Antennas Wirel. Propag. Lett. 2014;13:411–414.
10. Balanis CA. Antenna theory, analysis and design., 3rd ed. New Jersey: John Wiley & Sons; 2016.
11. Pozar DM. Microwave engineering, 4th ed. New York: John Wiley &Sons, Inc. 2012:1–756.
12. Mathworks User's Guide. MATLAB Documentation; 2021. [Online].
    Available:www.mathworks.com/help/pdf_doc/gads/gads_tb.pdf.
    Access on 10-Jan-2021
13. Chen X, Zhang S and Li Q. A Review of mutual coupling in MIMO systems. IEEE Access. 2018;6:24706–24719.
14. Garg R, Bhartia P, Bahl I, Ittipiboon A. Microstrip antenna design handbook. Norwood, MA: Artech House; 2001.
15. Saurabh AK, Rathore PS, Meshram MK. Compact wideband four-element MIMO antenna with high isolation. Electron. Lett. 2020;56(3):117–119.
16. Hua Q, Huang Y, Song C, Akinsolu MO, Liu B, Jia T, Xu Q. A novel compact quadruple-band indoor base station antenna for 2G/3G/4G/5G Systems. IEEE Access. 2019;7:151350–151358.
17. Abubakar HS, Zhao Z, Wang B, Kiani SH, Parchin NO, Hakim B. Eight-port modified E-slot MIMO antenna array with enhanced isolation for 5G mobile phone. Electronics. 2023;12(2):316.
18. Kiani SH, Altaf A, Anjum MR, Afridi S, Arain ZA, Anwar S, Khan S, Alibakhshikenari M, Lalbakhsh A, Khan MA, et al. MIMO antenna system for modern 5G handheld devices with healthcare and high rate delivery. Sensors. 2021;21(21):7415.
19. Kiani SH, Altaf A, Abdullah M, Muhammad F, Shoaib N, Anjum MR, Damaševičius R, Blažauskas T. Eight element side edged framed MIMO antenna array for future 5G smart phones. Micromachines. 2020; 11(11):956.

20. Ali H, Ren X-C, Hashmi AM, Anjum MR, Bari I, Majid SI, Jan N, Tareen WUK, Iqbal A, Khan MA. An eight element dual band antenna for future 5G smartphones. Electronics. 2021;10(23): 3022.